The HELIUM code: an ab-initio full-dimensional integrator of the time-dependent Schrödinger equation for a two-electron atom or ion in an intense laser field

Laura Moore

Queen's University Belfast

Methods and Codes for Atoms and Molecules in Strong Laser Fields Workshop, 29 April 2011

Plan of Talk

- Introduction to HELIUM
- The PDE and the Algorithm
- The computational demand of HELIUM
- Post-processing capabilities
- Future plans
- Summary

HELIUM

Purpose:

To solve the time-dependent Schrödinger equation accurately for a two-electron atom or ion responding to intense laser light. Pioneering HPC code - started with Cray T3D.

Scientific area:

Atto-second Science - the time scale of electron motion in matter. 1 atto-second = 10^{-18} second. The Ti:sapphire laser at its fundamental wavelength ($\lambda \sim 800$ nm) is the work-horse of this new subject.

HELIUM

Demand:

HELIUM

Demand:

Memory. Grown from ~ 16 Gbytes on Cray T3D to ~ 15 Tbytes on Cray XE6

HELIUM

Demand:

Memory. Grown from ~ 16 Gbytes on Cray T3D to ~ 15 Tbytes on Cray XE6

Communications. Per 12 wall-clock hour run there are 100,000 transfer events each involving 50 Gbytes

Helium and a short intense laser pulse

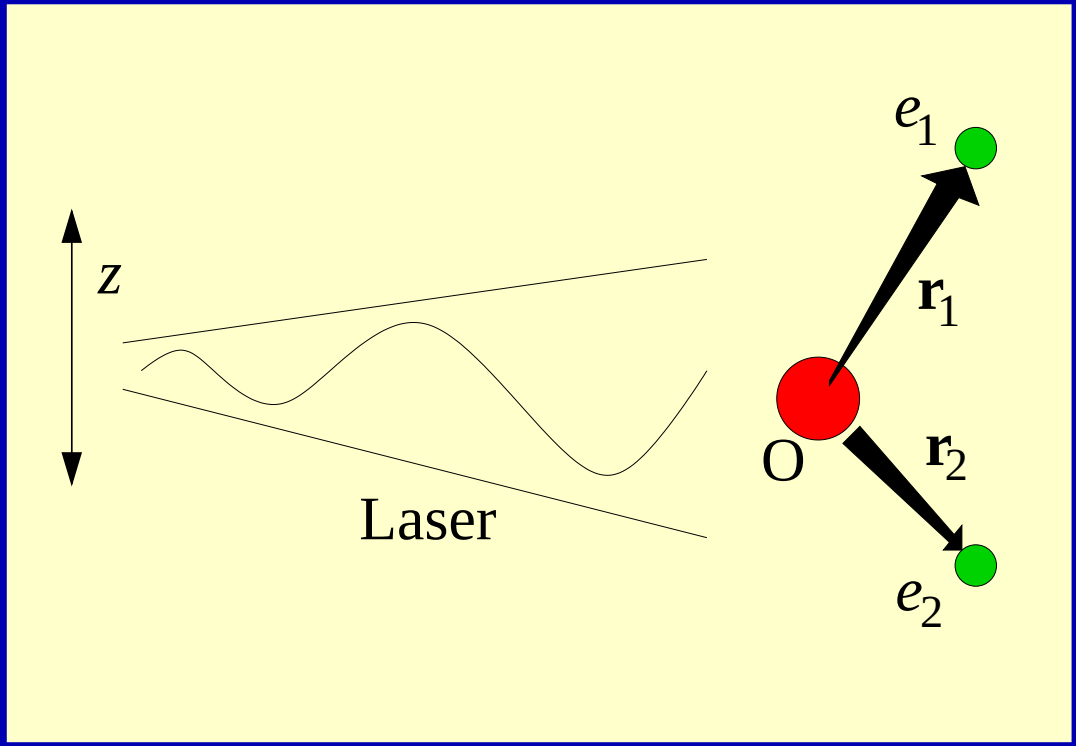

Helium atom plus intense laser

$$\mathrm{i}\frac{\partial \Psi}{\partial t} = H\Psi(\mathbf{r}_1, \mathbf{r}_2, t) \qquad \text{TDSE}$$

Fundamental equation of Quantum Mechanics

Atomic units $e = m = \hbar = 1$

Helium atom plus intense laser

$$\mathrm{i}\frac{\partial \Psi}{\partial t} = H\Psi(\mathbf{r}_1, \mathbf{r}_2, t) \qquad \text{TDSE}$$

Fundamental equation of Quantum Mechanics

$$\begin{aligned} H \;=\; & -\frac{1}{2}\nabla_1^2 - \frac{Z}{r_1} - \frac{A(t)}{\mathrm{i}\,c}\frac{\partial}{\partial z_1} \\ & + \frac{1}{r_{12}} \\ & - \frac{1}{2}\nabla_2^2 - \frac{Z}{r_2} - \frac{A(t)}{\mathrm{i}\,c}\frac{\partial}{\partial z_2} \end{aligned}$$

Atomic units $e = m = \hbar = 1$

Requirements

- Efficiency on massively parallel machines (minimum communications overhead)

- High accuracy (solution maintained correct to at least 13 decimal places)

Calculated (full-lines) and Ohio State measured (dashed-lines) momentum-resolved single- and double-ionization electron spectra for He exposed to 390 nm laser light

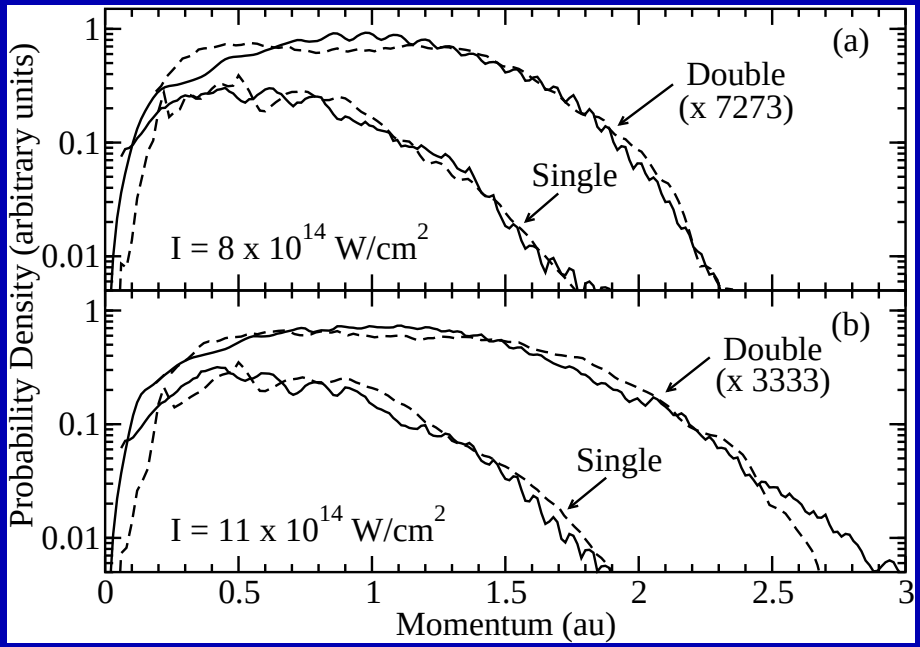

Solving the TDSE

- To solve $\dot{\Psi} = -\mathrm{i}H\Psi$ choose

$$\Psi = \sum_{\ell_1\,\ell_2\,L} \frac{1}{r_1 r_2} f_{\ell_1\ell_2 L}(r_1, r_2, t)\,|\ell_1\,\ell_2\,L\rangle$$

- Propagate over grid from $\Psi(\mathbf{r}_1, \mathbf{r}_2, t)$ to $\Psi(\mathbf{r}_1, \mathbf{r}_2, t + \delta t)$ using an Arnoldi propagator

Time propagation using an Arnoldi propagator

Time propagation (1)

- $\Psi(\mathbf{r_1}, \mathbf{r_2}, t)$ - propagate over a discrete time interval δt

$$\Psi(t + \delta t) = \Psi(t) + \delta t \dot{\Psi}(t) + \frac{(\delta t)^2}{2!} \ddot{\Psi}(t) + ...$$

Time propagation (1)

- $\Psi(\mathbf{r_1}, \mathbf{r_2}, t)$ - propagate over a discrete time interval δt

$$\Psi(t+\delta t) = \Psi(t) + \delta t \dot{\Psi}(t) + \frac{(\delta t)^2}{2!}\ddot{\Psi}(t) + ...$$

- But $\dot{\Psi} = -\mathrm{i}H\Psi$, where H is a very large sparse matrix, and so

$$\Psi(t+\delta t) = \mathrm{e}^{-\mathrm{i}H\delta t}\Psi(t)$$

Time propagation (2)

- To n^{th} order the Taylor series propagation is

$$\Psi_{\mathrm{TS}}(t+\delta t) = \sum_{k=0}^{n} \frac{(-\mathrm{i}\delta t)^k}{k!} H^k \Psi$$

Time propagation (2)

- To n^{th} order the Taylor series propagation is

$$\Psi_{\mathrm{TS}}(t+\delta t) = \sum_{k=0}^{n} \frac{(-\mathrm{i}\delta t)^k}{k!} H^k \Psi$$

- The Krylov sub-space K_{n+1} is the sub-space spanned by vectors $\Psi, H\Psi, \ldots, H^n\Psi$.

Krylov subspace (1)

- Space spanned by the vectors $\Psi, H\Psi, \ldots, H^n\Psi$

Krylov subspace (1)

- Space spanned by the vectors $\Psi, H\Psi, ..., H^n\Psi$
- Gram-Schmidt orthogonalization of these yields $n+1$ ortho-normal vectors $Q_0, Q_1, ..., Q_n$ collected as columns of a non-square matrix Q

Krylov subspace (1)

- Space spanned by the vectors $\Psi, H\Psi, ..., H^n\Psi$
- Gram-Schmidt orthogonalization of these yields $n+1$ ortho-normal vectors $Q_0, Q_1, ..., Q_n$ collected as columns of a non-square matrix Q
- Then the Arnoldi propagation is

$$\Psi_{\mathrm{AP}}(t+\delta t) = Q\mathrm{e}^{-\mathrm{i}h\delta t}Q^\dagger\Psi(t)$$

where $h = Q^\dagger HQ$ is a tri-diagonal square matrix of order $n+1$ of G-S coefficients.

Arnoldi Propagator: H and Q matrices

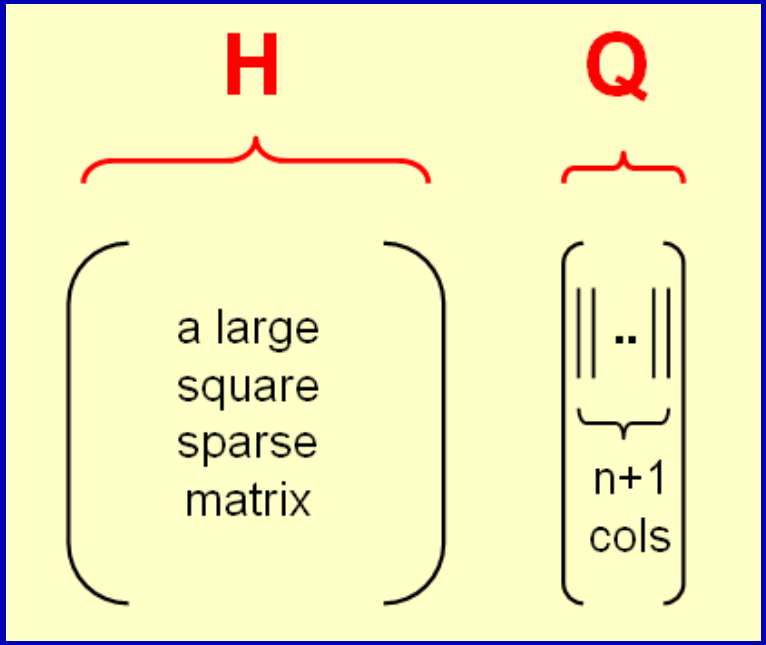

Order of H is typically 58×10^9

Value of n is typically 15

Krylov subspace (2)

- From $h = Q^\dagger H Q$ where h is of order $n+1$ we have

$$\tilde{H} = Q h Q^\dagger$$

Krylov subspace (2)

- From $h = Q^\dagger H Q$ where h is of order $n+1$ we have

$$\tilde{H} = Q h Q^\dagger$$

- Moreover since $(Q h Q^\dagger)^m = Q h^m Q^\dagger$ then

$$\mathrm{e}^{-\mathrm{i}\tilde{H}\delta t} = Q \mathrm{e}^{-\mathrm{i}h\delta t} Q^\dagger$$

where $Q\mathrm{e}^{-\mathrm{i}h\delta t}Q^\dagger$ is the Arnoldi propagator, viz:

$$\Psi_{\mathrm{AP}}(t+\delta t) = \mathrm{e}^{-\mathrm{i}\tilde{H}\delta t} = Q \mathrm{e}^{-\mathrm{i}h\delta t} Q^\dagger \Psi(t)$$

Five benefits of the Arnoldi propagator

- It is explicit - vital for massively parallel machines
- Computational overhead rises linearly with n
- A unitary operator correct to order n in δt
- Very efficient way to obtain Hamiltonian eigenstates
- At least twice as efficient as Taylor series and performance ratio scales linearly with n

Computational demand of HELIUM

Time-propagating the wavefunction

- $$\Psi = \sum_{\ell_1\,\ell_2\,L} \frac{1}{r_1 r_2} f_{\ell_1 \ell_2 L}(r_1, r_2, t)\,|\ell_1\,\ell_2\,L\rangle$$

- Propagate over grid from $\Psi(\mathbf{r}_1, \mathbf{r}_2, t)$ to $\Psi(\mathbf{r}_1, \mathbf{r}_2, t + \delta t)$ using an Arnoldi propagator

Length of vector $f_{\ell_1' \ell_2' L'}(r_1, r_2, t)$ at any t

- For necessary accuracy, our biggest calculations so far (for Ti:sapphire laser $\lambda = 800$ nm) using $16,110$ HECToR cores have demanded:
  - About 2,000 distinct ℓ_1, ℓ_2, L triplets
  - Typically 5,370 mesh points in each of r_1 and r_2

Length of vector $f_{\ell_1' \ell_2' L'}(r_1, r_2, t)$ at any t

- For necessary accuracy, our biggest calculations so far (for Ti:sapphire laser $\lambda = 800$ nm) using $16,110$ HECToR cores have demanded:
  - About 2,000 distinct ℓ_1, ℓ_2, L triplets
  - Typically 5,370 mesh points in each of r_1 and r_2
- Hence length of f is
  $\sim 2 \times 10^3 \times 5 \times 10^3 \times 5 \times 10^3 = 57.7 \times 10^9$
  $= 922$ Gbytes memory.

Length of vector $f_{\ell_1' \ell_2' L'}(r_1, r_2, t)$ at any t

- For necessary accuracy, our biggest calculations so far (for Ti:sapphire laser $\lambda = 800$ nm) using $16,110$ HECToR cores have demanded:
  - About 2,000 distinct ℓ_1, ℓ_2, L triplets
  - Typically 5,370 mesh points in each of r_1 and r_2
- Hence length of f is
  $\sim 2 \times 10^3 \times 5 \times 10^3 \times 5 \times 10^3 = 57.7 \times 10^9$
  $= 922$ Gbytes memory.
- to time propagate, we need approx. 16 vectors of such length - $\sim 14,752$ Gybtes

Computer code design

fortran90 + MPI: Distribution over cores

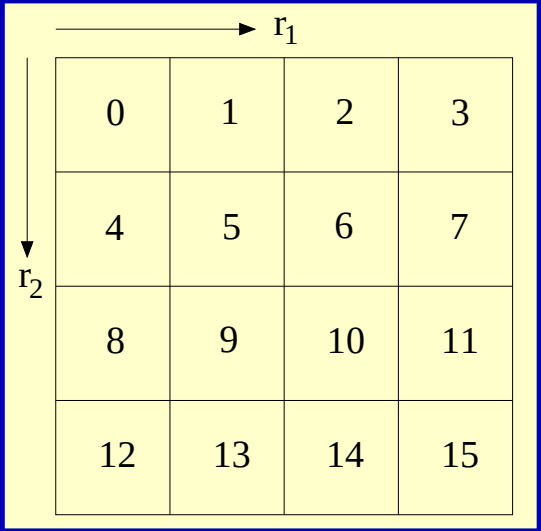

Illustrative 16 core example

- Each core is assigned a region of r_1, r_2 space

fortran90 + MPI: Distribution over cores

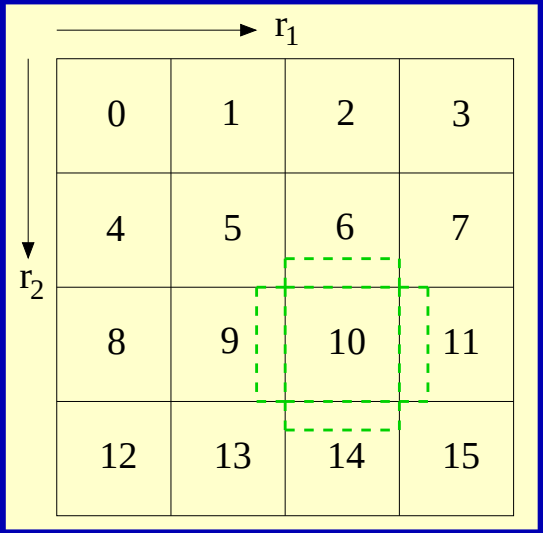

Illustrative 16 core example

- Each core is assigned a region of r_1, r_2 space
- Each region has to communicate with neighbouring regions (boundary swapping)

fortran90 + MPI: Distribution over cores

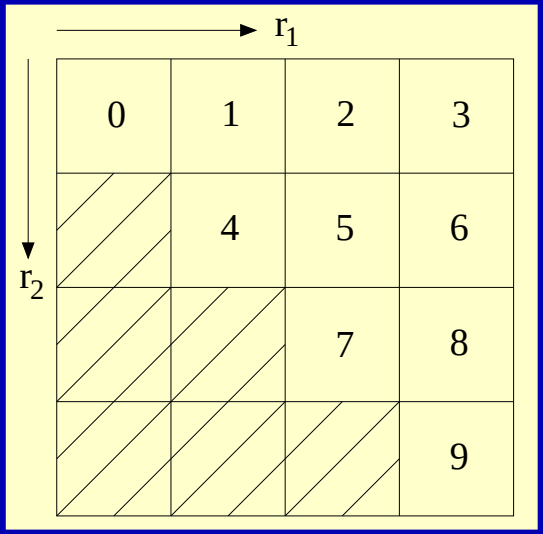

Illustrative 10 core example

- The problem is symmetrical $\Rightarrow$ Saving on core count

fortran90 + MPI: Distribution over cores

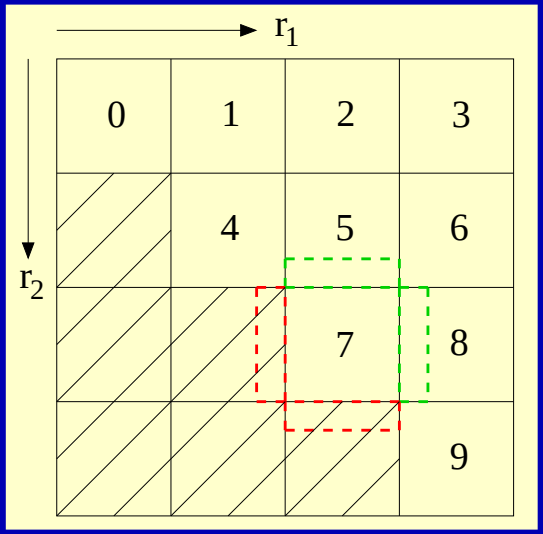

Illustrative 10 core example

- The problem is symmetrical $\Rightarrow$ Saving on core count
- Care must be taken while boundary swapping

Communications

- Communications occur $\sim 100,000$ times per 12-hour run
- Each communication transfers ~ 50 Gbytes of data
- On the Cray XE6 such communications occupy only 5% of running time!

Ti:sapphire $\lambda = 800$ nm calculations using near full capability of EPCC Cray XE6

Ti:sapphire $\lambda = 800$ nm calculations using near full capability of EPCC Cray XE6

Motivation: Much experimental data at 800 nm

1D 3-step recollision mechanism for double ionization

- Step 1 - field ionization of first electron
- Step 2 - this first electron moves away from the nucleus but is subsequently driven back, by the laser field, towards the parent core. The first electron then recollides with the parent core and at the instant of recollision has a maximum energy of 3.2 U_p.
- Step 3 - the recollision brings about double ionization

Joint momentum-space probability distribution at 390 nm

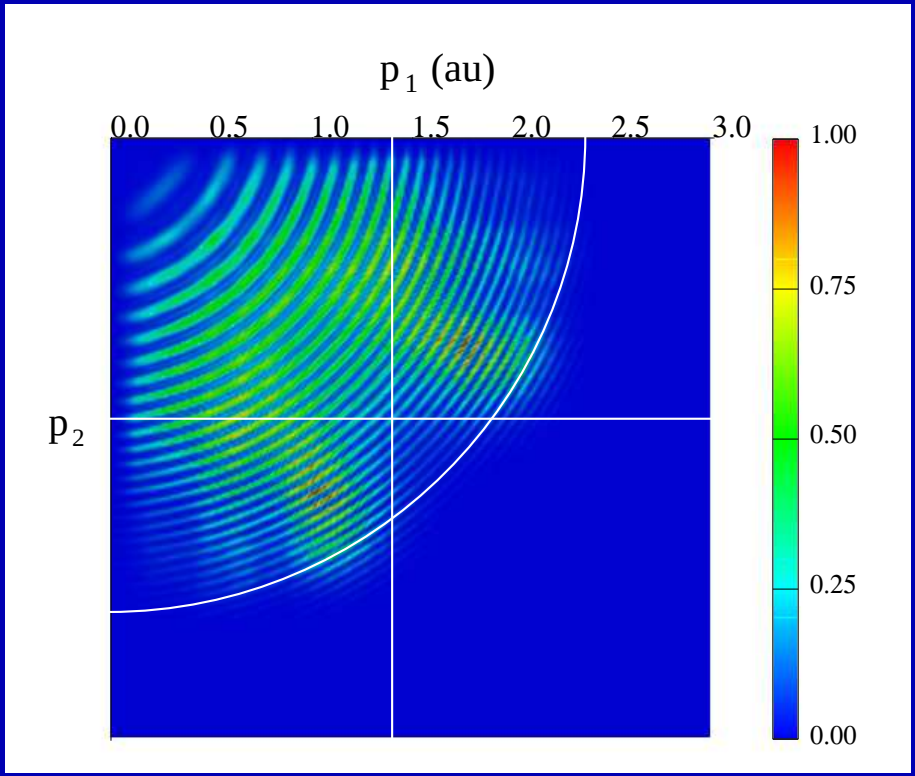

Prediction verified by laboratory experiment

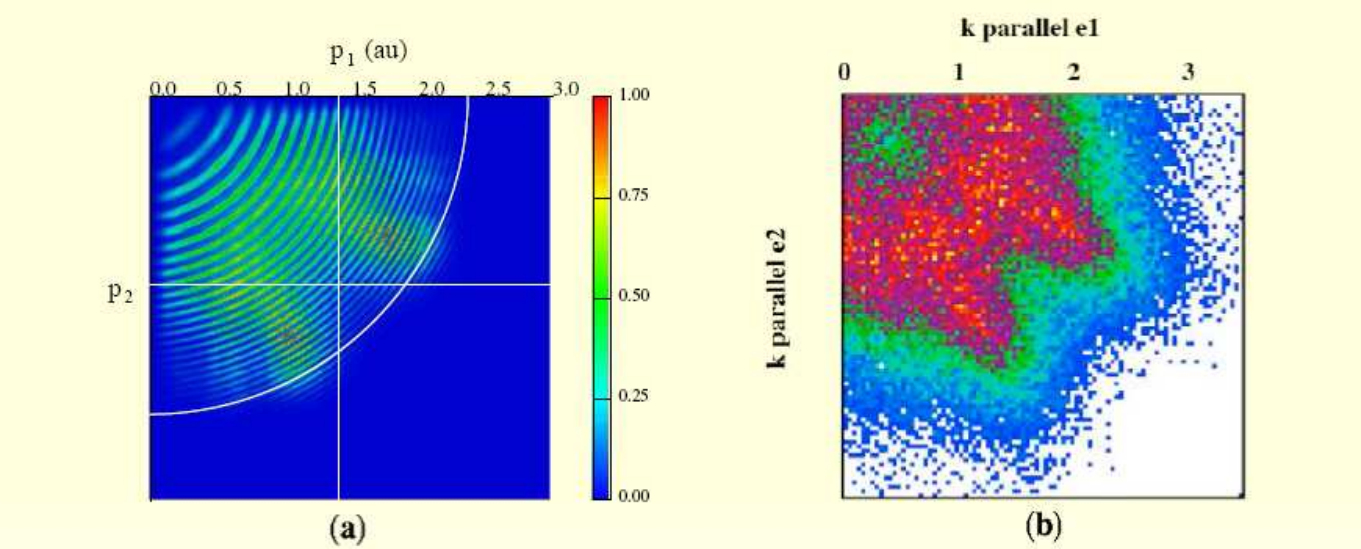

(a) This work 390 nm, 10 $\times 10^{14}$ W/cm^2

Parker *et al* PRL **96** 133001 (2006)

(b) Experimental 800 nm, 4.5 $\times 10^{14}$ W/cm^2

Staudte *et al* PRL **99** 263002 (2007)

800 nm Run Size

- 16,110 cores
- 108 wallclock hours per pulse (nine 12-hour runs)
- 9-cycle laser pulse

Plot of two-electron radial momentum space probability density at end of 7-cycle laser pulse, peak intensity 3.2×10^{14} W/cm^2 at 800 nm. The colour scale is linear.

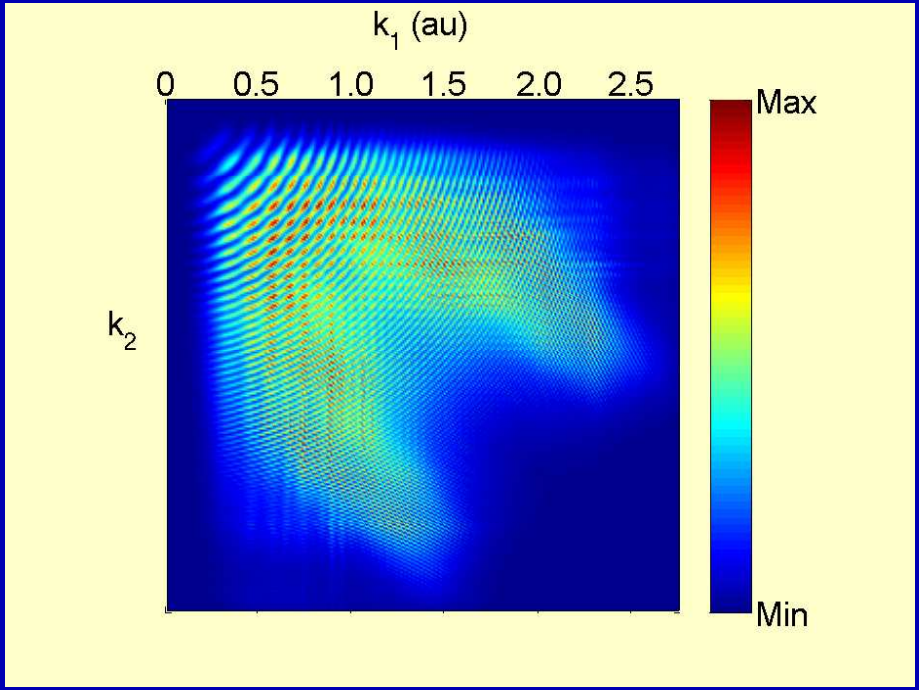

Results at 800 nm

Results at 800 nm

- Cut-off in the total KE:

$$\text{at low } I \quad : \quad 5\,U_p(\ I \text{ independent})$$

$$I > 2.2 \times 10^{14}\ \mathrm{W/cm^2} \quad : \quad 5 \text{ to } 8\,U_p(\ I \text{ dependent})$$

Results at 800 nm

- Cut-off in the total KE:

$$\text{at low } I \quad : \quad 5\,U_p(\ I \text{ independent})$$

$$I > 2.2 \times 10^{14}\ \mathrm{W/cm^2} \quad : \quad 5 \text{ to } 8\,U_p(\ I \text{ dependent})$$

- What's 2.2×10^{14} W/cm^2?

  The classical recollisional excitation threshold at 800 nm.

Results at 800 nm

- Cut-off in the total KE:

$$\text{at low } I \quad : \quad 5\,U_p(\ I \text{ independent})$$

$$I > 2.2 \times 10^{14}\ \mathrm{W/cm^2} \quad : \quad 5 \text{ to } 8\,U_p(\ I \text{ dependent})$$

- What's 2.2×10^{14} W/cm^2?

  The classical recollisional excitation threshold at 800 nm.

- Analysis ongoing!

Post-processing of wavefunction

Radial probability density

- $$\Psi = \sum_{\ell_1\,\ell_2\,L} \frac{1}{r_1 r_2} f_{\ell_1 \ell_2 L}(r_1, r_2, t)\,|\ell_1\,\ell_2\,L\rangle$$

- Two-electron radial probability density

$$P(r_1, r_2, t) = \sum_{\ell_1\,\ell_2\,L} |f_{\ell_1 \ell_2 L}(r_1, r_2, t)|^2$$

Transformation of the final-state two-electron wavefunction into momentum-space

Momentum Representation

$$g(\mathbf{k}_1, \mathbf{k}_2, T_{\rm end})$$
$$= \int\int \Psi(\mathbf{r}_1, \mathbf{r}_2, T_{\rm end})\, X(\mathbf{r}_1, \mathbf{k}_1, \mathbf{r}_2, \mathbf{k}_2)\, {\rm d}\mathbf{r}_1 {\rm d}\mathbf{r}_2$$
$$= \sum_{\ell_1\, \ell_2\, L} \frac{1}{k_1\, k_2} g_{\ell_1 \ell_2 L}(k_1, k_2, T_{\rm end}) |\ell_1\, \ell_2\, L>$$

Hence

$$P_{\rm mom}(k_1, k_2, T_{\rm end}) = \sum_{\ell_1\, \ell_2\, L} |g_{\ell_1 \ell_2 L}(k_1, k_2, T_{\rm end})|^2$$

Application to 2-photon double-ionization of Helium

Theoretical calculations of non-sequential double-ionization (NSDI) cross-sections differ by an order of magnitude.

2-photon NSDI cross-sections

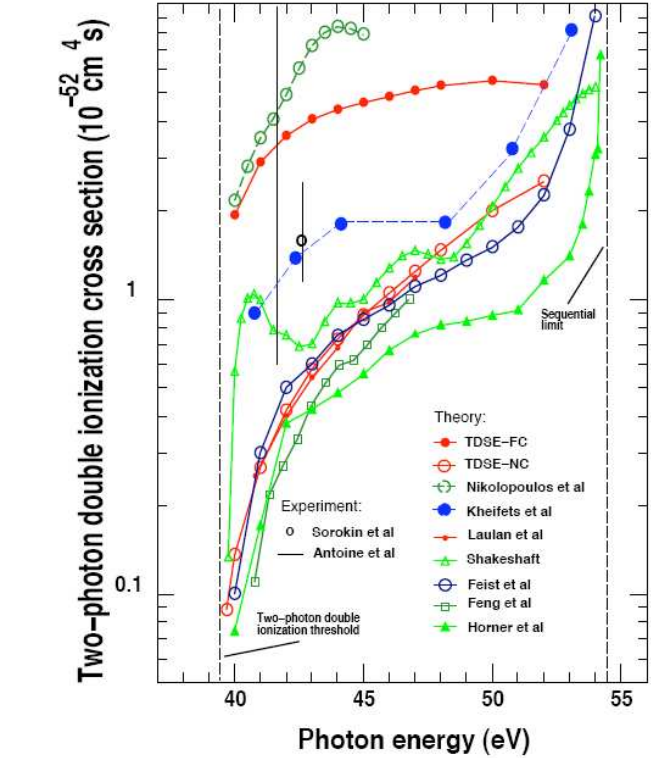

(taken from B Piraux *et. al.* J Phys: Conf Series **141** 012013 (2008))

HELIUM Calculation of 2-photon NSDI cross-sections

- Choose low intensity (10^{13} W/cm^2) so as to minimize sequential ionization.
- Choose laser frequency of 1.6 a.u. (43.5 eV).
- 2-photon double-ionization is a direct process

Energy level diagram of He

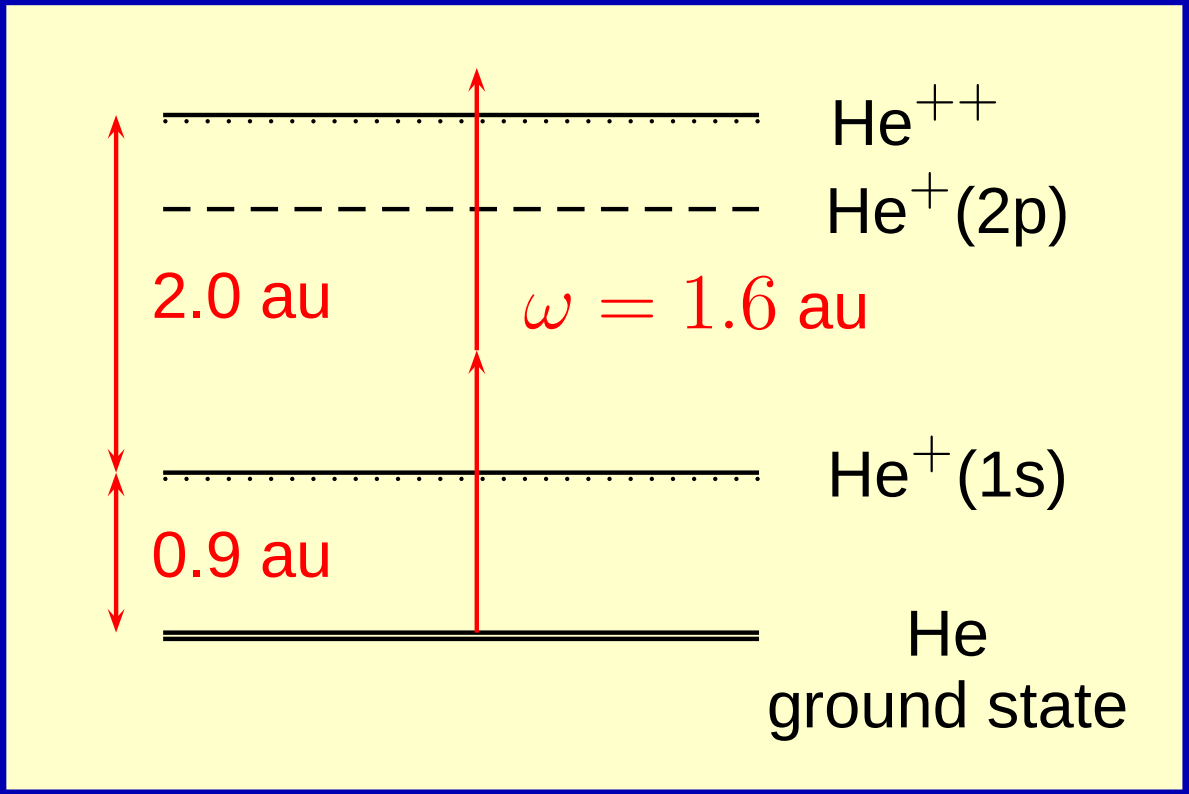

Run parameters

- $l_{1,2\ \mathrm{max}}$ = 4 (~ 100 basis states)
- $\delta r = 0.29$ a.u.
- 4200 grid points for r_1 and r_2 (integration extends to 1218 Bohr radii)
- Pulse ramp-on 18 T, constant for 30 T, ramp-off 18 T.
- Calculation runs for a further 30 T (field-free) to let doubly-ionizing electrons depart the strong Coulomb field of the residual ion.

Radial probability distribution right after laser pulse has ramped off

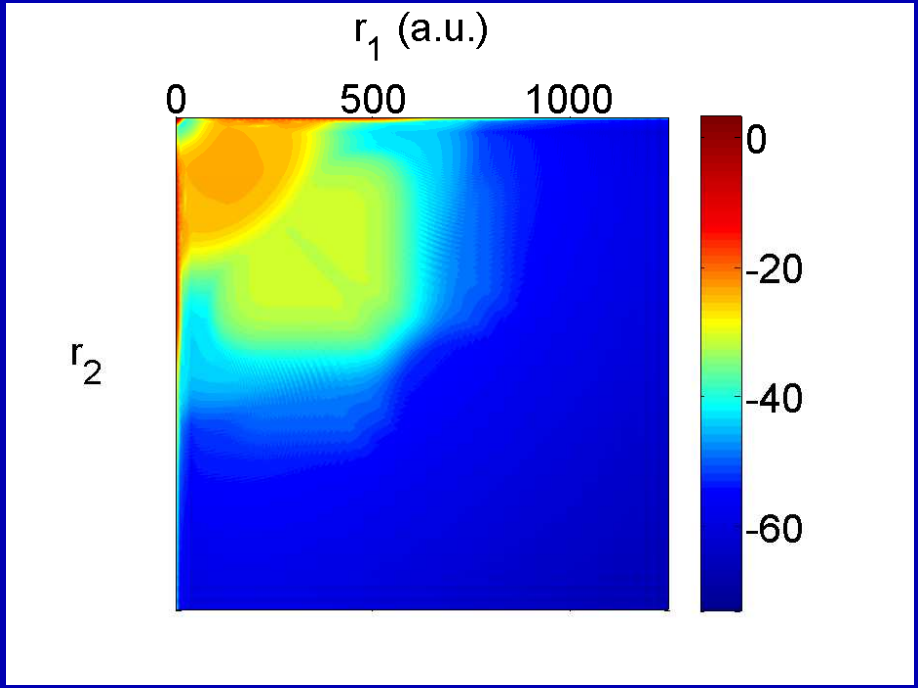

Radial probability distribution a further 30 T after the laser pulse has ramped off

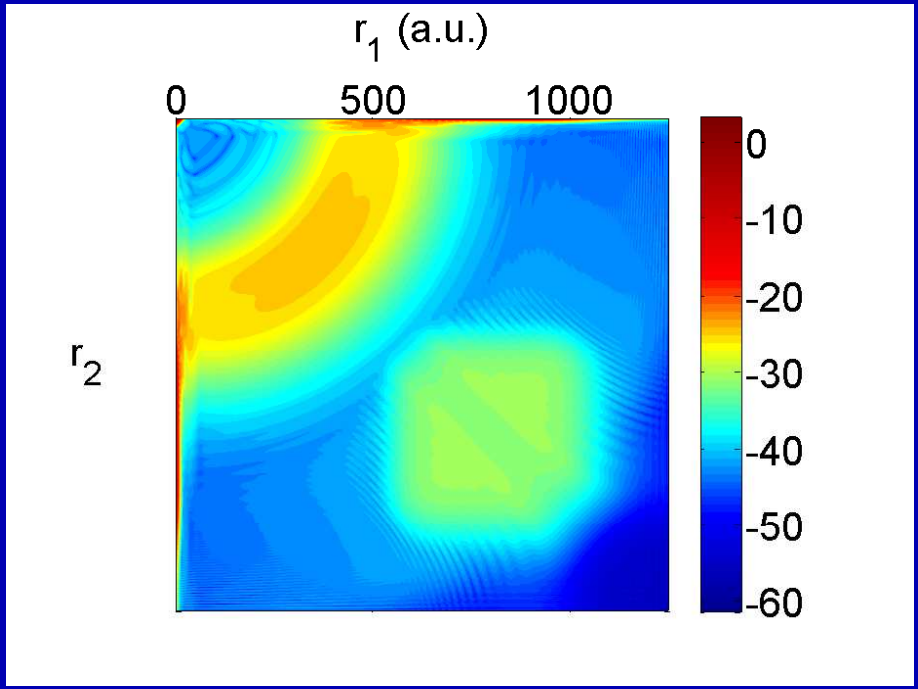

Joint momentum-space probability distribution of the two doubly-ionizing electrons obtained by projecting the final-state wavefunction onto plane waves

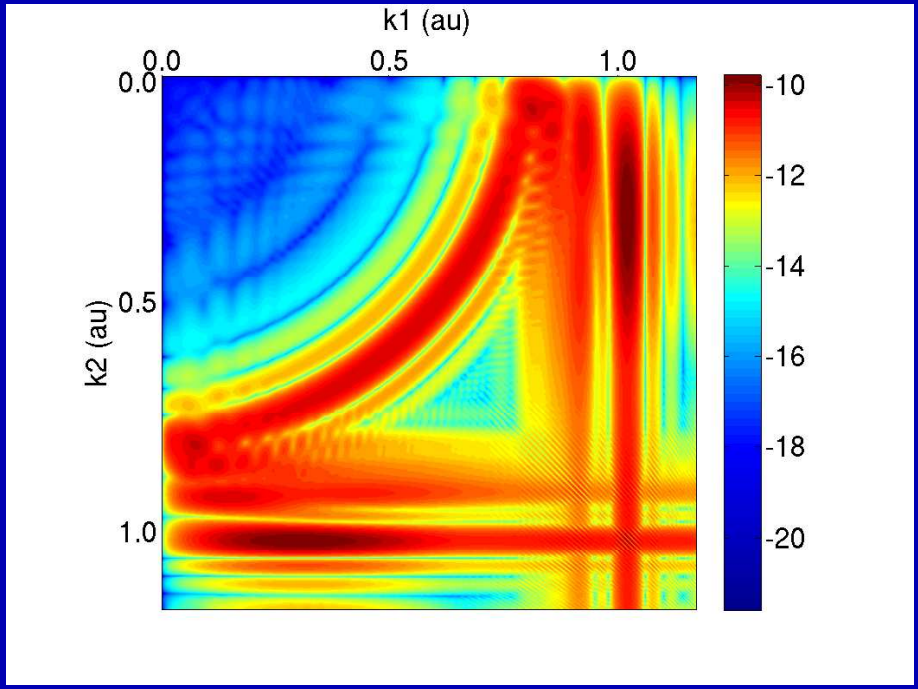

Joint momentum-space probability distribution at 390 nm

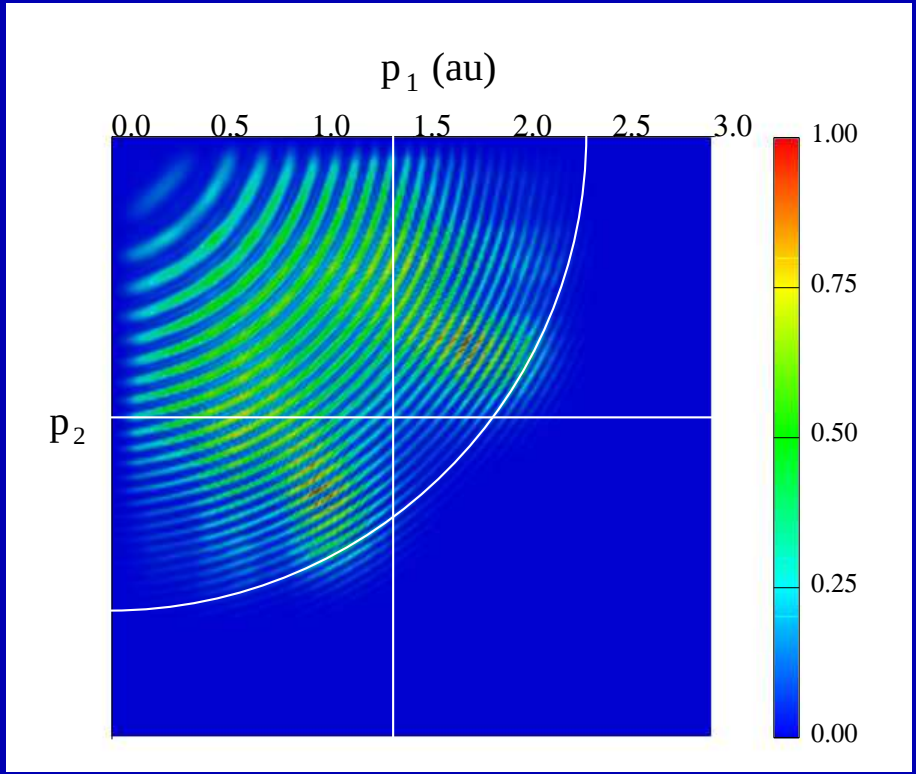

Joint momentum-space probability distribution at 390 nm

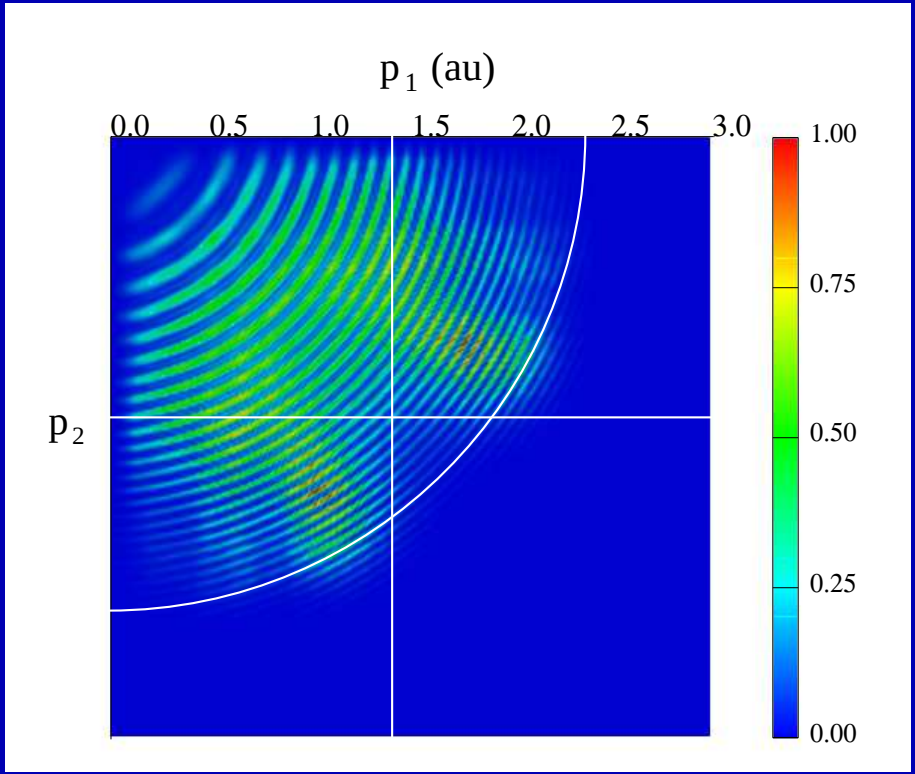

No rectilinear features!

Joint momentum-space probability distribution of the two doubly-ionizing electrons obtained by projecting the final-state wavefunction onto plane waves

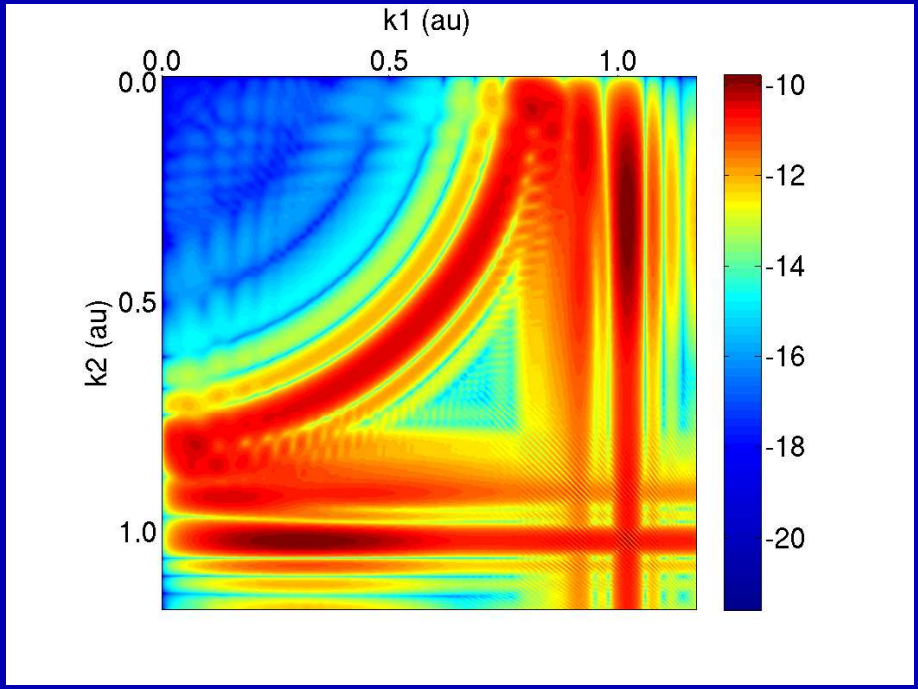

Calculation of 2-photon double-ionization cross-section

Calculation of 2-photon double-ionization cross-section

- No natural division between the arc and the linear features that represent bound states of He^{+}.

Calculation of 2-photon double-ionization cross-section

- No natural division between the arc and the linear features that represent bound states of He^{+}.

- Probability of 2-photon ionization as extracted from such a plot can vary by up to a factor of 1.5.

Calculation of 2-photon double-ionization cross-section

- No natural division between the arc and the linear features that represent bound states of He^+.
- Probability of 2-photon ionization as extracted from such a plot can vary by up to a factor of 1.5.
- Need to remove single ionization contributions (by projecting onto eigenstates of He^+).

Projecting out singly ionizing states

Projecting out singly ionizing states

- Very high accuracy in the treatment of the He^+ bound states is essential.

Projecting out singly ionizing states

- Very high accuracy in the treatment of the He^+ bound states is essential.
- He^+ bound states obtained through eigen-decomposition of the field-free finite-difference Hamiltonian.

Projecting out singly ionizing states

- Very high accuracy in the treatment of the He^+ bound states is essential.
- He^+ bound states obtained through eigen-decomposition of the field-free finite-difference Hamiltonian.
- Eigenvectors calculated using a Lanczos/Arnoldi method on a discrete finite-difference grid.

Projecting out singly ionizing states

- Very high accuracy in the treatment of the He^+ bound states is essential.
- He^+ bound states obtained through eigen-decomposition of the field-free finite-difference Hamiltonian.
- Eigenvectors calculated using a Lanczos/Arnoldi method on a discrete finite-difference grid.
- All components of the spatial final-state wavefunction in the directions of these orthogonal bound states are removed.

After removing all singly ionizing components of the spatial final-state wavefunction, project onto plane waves

Joint momentum-space probability distribution obtained by projecting onto plane waves:

(a) the final-state wavefunction

(b) the final-state wavefunction after removal of He^+ bound states

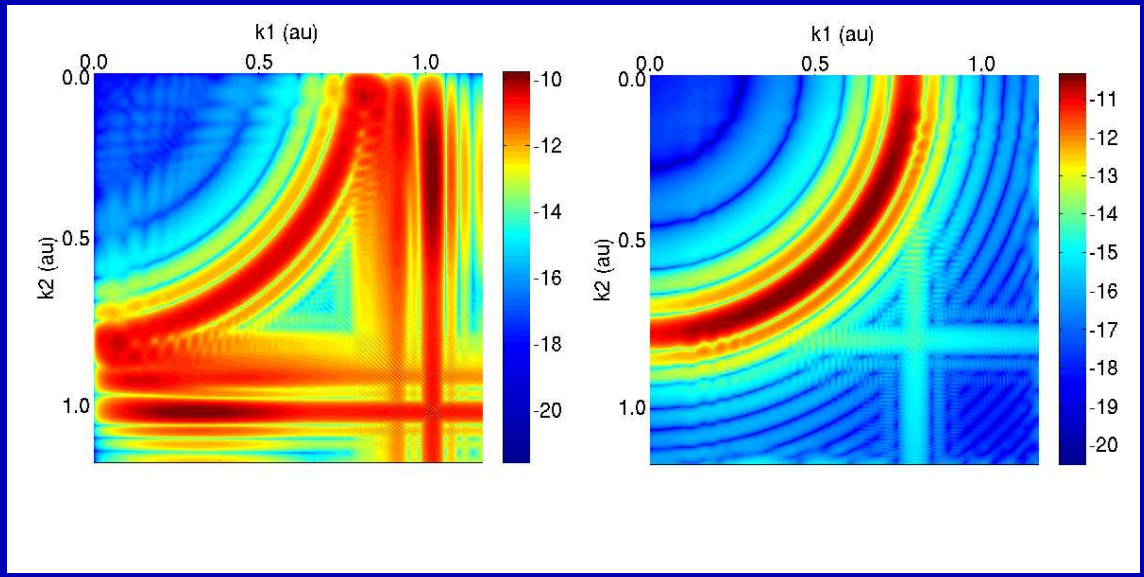

(a) (b)

A further check ...

- Remove components from the spatial wavefunction $\Psi(\mathbf{r_1}, \mathbf{r_2}, T)$ involving bound states of the residual He^+ ion.

- Project remainder onto a basis of Coulomb states.

Joint momentum-space probability distribution obtained by projecting onto Coulomb waves the final-state wavefunction after removal of He^+ bound states

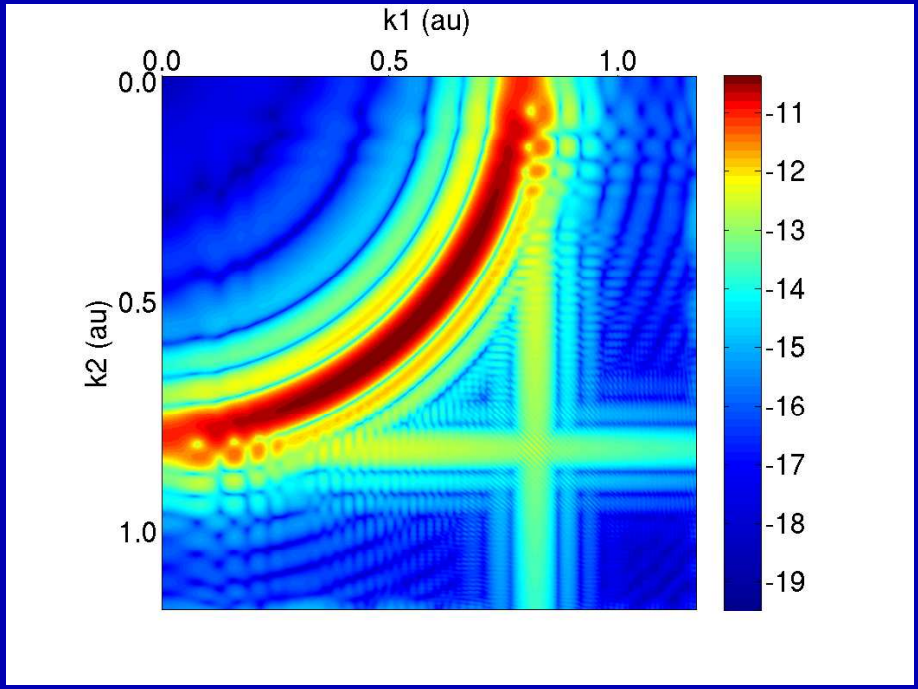

Joint momentum-space probability distribution obtained by projecting the final-state wavefunction, after removal of He^+ bound states, onto:

(a) Plane waves

(b) Coulomb waves

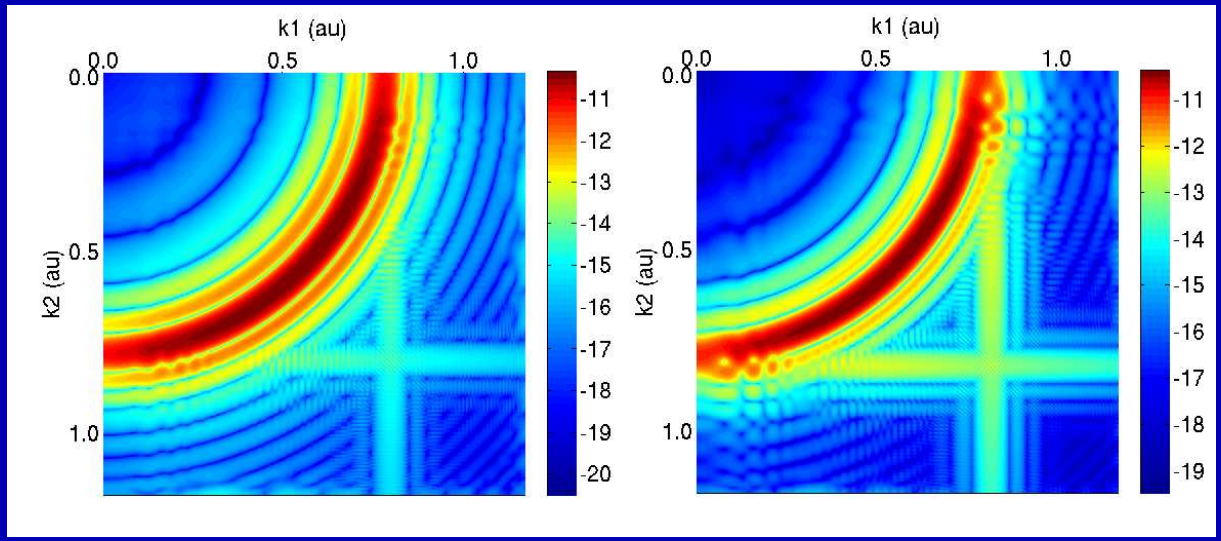

(a) (b)

HELIUM 2-photon NSDI cross-section at $\omega = 1.6$ a.u. (43.5 eV)

HELIUM 2-photon NSDI cross-section at $\omega = 1.6$ a.u. (43.5 eV)

- Any remaining linear feature now contains negligible population.

HELIUM 2-photon NSDI cross-section at $\omega = 1.6$ a.u. (43.5 eV)

- Any remaining linear feature now contains negligible population.
- Both methods (projection onto plane waves and onto Coulomb waves) give same cross-section to within 3%.

HELIUM 2-photon NSDI cross-section at $\omega = 1.6$ a.u. (43.5 eV)

- Any remaining linear feature now contains negligible population.
- Both methods (projection onto plane waves and onto Coulomb waves) give same cross-section to within 3%.
- HELIUM cross-section value is 7.6×10^{-53} cm^{4}s

HELIUM 2-photon NSDI cross-section at $\omega = 1.6$ a.u. (43.5 eV)

- Any remaining linear feature now contains negligible population.
- Both methods (projection onto plane waves and onto Coulomb waves) give same cross-section to within 3%.
- HELIUM cross-section value is 7.6×10^{-53} cm^{4}s
- Still to test effects of some parameters (pulse shape).

2-photon NSDI cross-sections

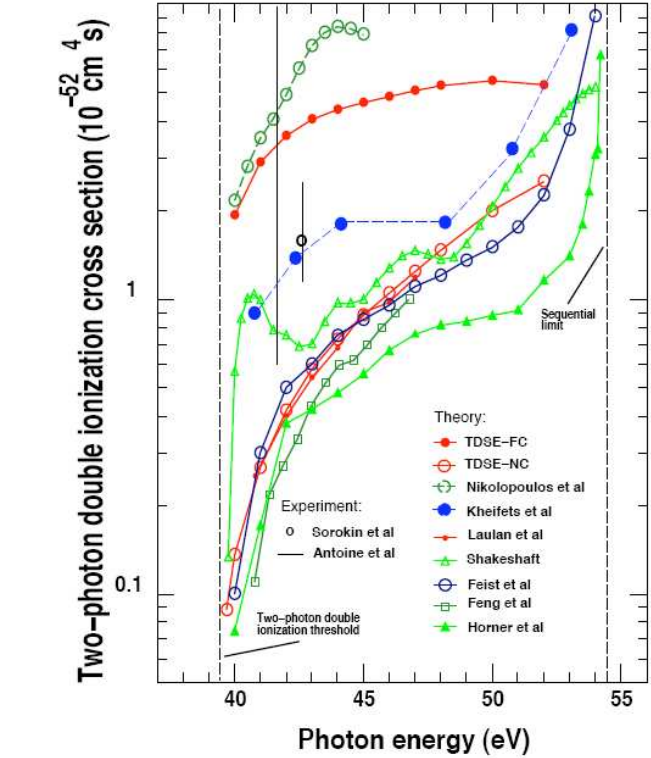

(taken from B Piraux *et. al.* J Phys: Conf Series **141** 012013 (2008))

2-photon NSDI cross-sections

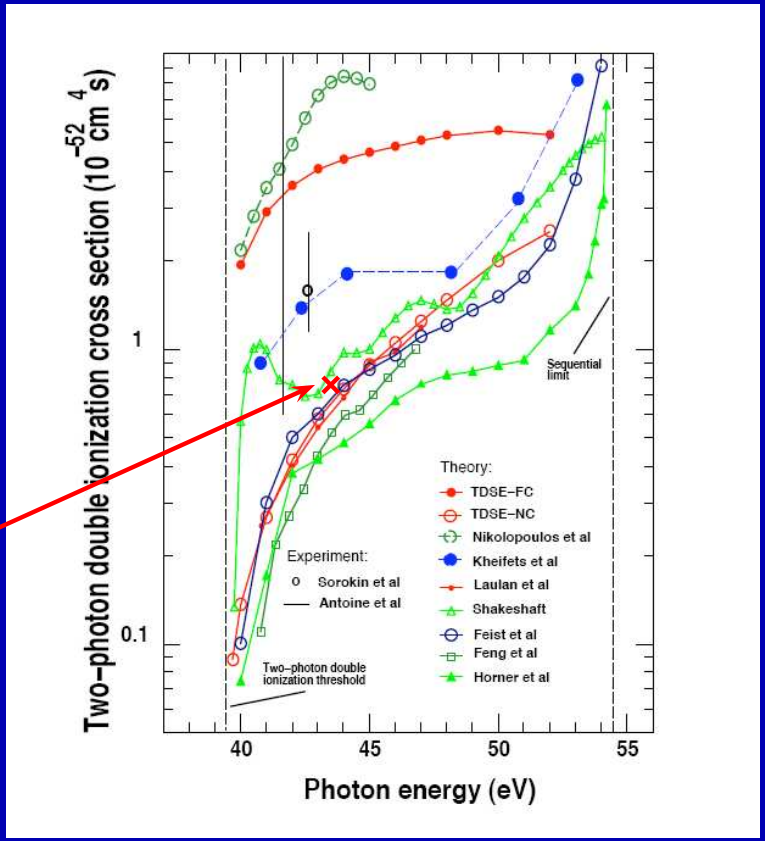

HELIUM

(taken from B Piraux *et. al.* J Phys: Conf Series **141** 012013 (2008))

HELIUM 2-photon NSDI cross-section calculations

- HELIUM cross-section at $\omega = 1.6$ a.u. (43.5eV) in the thicket!
- Still to test effects of some parameters (pulse shape).
- Intend to calculate cross-sections at other photon energies too.

New extensions to HELIUM

New extensions to HELIUM

- Non-dipole interactions

New extensions to HELIUM

- Non-dipole interactions
  - Enables calculations to be carried out at x-ray wavelengths.
  - M is not conserved, so basis set has been extended from $|\ell_1\, \ell_2\, L\rangle$ to $|\ell_1\, \ell_2\, L, M\rangle$.
  - New Hamiltonian terms.

New extensions to HELIUM

New extensions to HELIUM

- Crossed laser fields

New extensions to HELIUM

- Crossed laser fields
  - Enables calculations to be carried out with two perpendicular laser fields (with two arbitrary frequencies), or with one laser field of circular/elliptic polarization.
  - M is not conserved, so basis set has been extended from $|\ell_1\, \ell_2\, L\rangle$ to $|\ell_1\, \ell_2\, L, M\rangle$.
  - New Hamiltonian terms.

A new post-processing code

A new post-processing code

- Transformation of wavefunction from spherical to cylindrical geometry.

A new post-processing code

- Transformation of wavefunction from spherical to cylindrical geometry.
  - Enables direct comparison with data from many experiments.

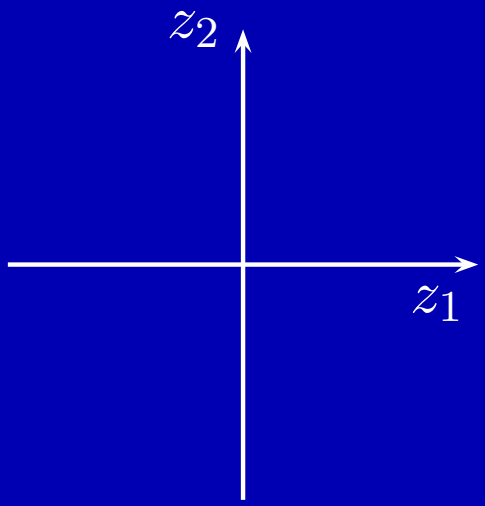

Future plans

Carry over of HELIUM Methods

Carry over of HELIUM Methods

- There is a crucial need to handle the TDSE accurately for multi-electron atoms and molecules coupled to IR/visible/UV and VUV laser fields and undergoing double- and/or single-ionization.

Carry over of HELIUM Methods

- There is a crucial need to handle the TDSE accurately for multi-electron atoms and molecules coupled to IR/visible/UV and VUV laser fields and undergoing double- and/or single-ionization.
- The R-matrix concept allows the carry over of HELIUM methods – development of the RMT (R-Matrix incorporating Time) code – next talk by Michael Lysaght.

People currently working directly with HELIUM

- Ken Taylor
- Jonathan Parker
- Laura Moore
- Gregory Armstrong
- David Robinson

Acknowledgments

- UK EPSRC

- The distributed Computational Science and Engineering service operated by the Numerical Algorithms Group Ltd

Summary

Summary

- The Arnoldi propagator has allowed us to handle the high-dimensionality TDSE for two-electron atoms in intense laser fields efficiently and to the accuracy necessary to complement laboratory experiment.

Summary

- The Arnoldi propagator has allowed us to handle the high-dimensionality TDSE for two-electron atoms in intense laser fields efficiently and to the accuracy necessary to complement laboratory experiment.
- The EPCC Cray XE6 (HECToR) with this propagator in use has allowed first double-ionization spectra to be calculated for fundamental Ti:sapphire laser light.

Summary

- The Arnoldi propagator has allowed us to handle the high-dimensionality TDSE for two-electron atoms in intense laser fields efficiently and to the accuracy necessary to complement laboratory experiment.
- The EPCC Cray XE6 (HECToR) with this propagator in use has allowed first double-ionization spectra to be calculated for fundamental Ti:sapphire laser light.
- Separating degenerate doubly and singly ionizing states in the final-state wavefunction has enabled calculation of 2-photon NSDI cross-sections with quantitative accuracy.

And finally!

And finally!

The HELIUM methods are being carried over to multi-electron atoms and molecules: the RMT (R-Matrix incorporating Time) code – next talk by Michael Lysaght.

And finally!

The HELIUM methods are being carried over to multi-electron atoms and molecules: the RMT (R-Matrix incorporating Time) code – next talk by Michael Lysaght.

Thanks for listening.